Exactness of source analysis of biomagnetic signals of epileptiform spikes by the method of spatial filtering: a computer simulation

H. Wagner M. Eiselt U. Zwiener

Institute of Pathological Physiology, Klinikum Friedrich Schiller Universität, D-07740 Jena, Germany

Abstract—*On the basis of spatial covariance, it is found that, by spatial filtering the localisation of a single dipole source, both parallel and perpendicular to the measurement plane (assuming a signal–noise ratio of 5:1), can be performed with an accuracy of < 0.5 mm. When the signal–noise ratio is increased to 30:1, the resolution of temporally independent current sources separated by 2 mm becomes practicable. This resolution study is carried out by means of a pair of unity current dipoles with the dipole distance as a varying source model parameter. The conclusions, drawn from the results of computer simulation and supported by statistical calculations, refer to the spherical model of the volume conductor of the brain.*

Keywords—*Source analysis, Spatial filter, MEG, SVD*

Med. Biol. Eng. Comput., 1997, **35**, 708–714

1 Introduction

THE MATHEMATICAL method of spatial filtering is a useful tool for the detection of electric sources in the brain from MEG data. It is particularly suited to analysis of magnetic fields with multiple sources, i.e. in the detection of both multiple discrete and spatially extended sources. With respect to the influence of sources outside the investigated source region, this method is relatively insensitive (ROBINSON and ROSE, 1992; GRUMMICH *et al.*, 1993). In addition, it allows the construction of a rough view of the distribution of sources in the source region under consideration before a more detailed source analysis is carried out.

Non-linear least squares estimations are used preferentially for the localisation of a single current source. For the localisation of multiple, spatially separated sources, the results of this estimation may be sensitive to the initial values of the parameters to be estimated (ACHIM *et al.*, 1991). Thus, for consistent estimation, efficient initial values are derived by means of a single value decomposition (BAUMGARTNER *et al.*, 1991). Apart from the method of spatial filtering and the non-linear least squares technique, alternative methods such as the MUSIC algorithm (STOICA and NEHORAI, 1989) or methods calculating a spatial current dipole field were chosen (IOANNIDES *et al.*, 1990). In contrast to the MUSIC algorithm, the spatial filtering method does not require any knowledge of the number of independent signal components, e.g. current dipoles (GREENBLATT, 1993).

Being a mathematically under-determined problem, a unique solution for the spatial dipole field is obtained according to the least squares-minimum norm principle (WANG *et al.*, 1993). This solution generally indicates a spatial blurring of discrete current sources. To find solutions that take into account extended sources in a better way, MRI information is involved in the reconstruction of the dipole field (FUCHS *et al.*, 1995). Instead of the minimum norm of the calculated current dipole field, the minimum norm of the 'source current density' of the dipole field has recently been introduced (PASCUAL-MARQUI *et al.*, 1994).

The aims of the work were:

(i) to examine the exactness of location of a single current source by spatial filtering of MEG data
(ii) to study the resolution of adjacent sources that can be best attained by the same method. This work deals in particular with the location of sources from the analysis of magnetic fields arising in connection with focal epileptic processes.

In the case of temporally dependent sources, the lower bounds of the separation of two discrete sources are known (MOSHER *et al.*, 1993). However, no investigations have been performed on independent sources, which are the subject of this paper. The relevance of the single dipole model in the analysis of a magnetic field that is generated by two adjacent dipoles or by a spatially distributed source has been studied by OKADA (1985). This work was also based on temporally dependent generators.

By taking measurements of the electric potential in animals caused by epileptiform activity it was found that the area of the penicillin-induced interictal spike activity in the cortex of the animal examined (rabbit) is located within a tissue volume with an extension of 3 mm vertically and less than 10×10 mm^2 horizontally (GOLDENSOHN *et al.*, 1995). Hence, to obtain relevant information on the spatio–temporal pattern of the neuro-electric processes accompanying the penicillin-induced interictal activity, the following requirements must be met: first, an accuracy of location of at least 1 mm must be

Correspondence should be addressed to Dr Wagner; email: ihw@hpux.rz.uni-jena.de.

First received 14 August 1995 and in final form 28 May 1997

ensured; secondly, the resolution, i.e. the spatial separation of adjacent sources, has to amount to at least 2 mm.

Up to now it has been known that:

(i) the location of sources in the human brain by means of magneto-encephalographic methods (squid technique) succeeds within a few millimetres at best (LÜTKENHÖNER, 1994; OGURA and SEKIHARA, 1993).
(ii) for adjacent dependent sources, a resolution is obtained that equals the distance between the source region and the plane of measurement (SHAOFEN *et al.*, 1990; LÜTKENHÖNER, 1994).

Single value decomposition analyses (SVD) of potential measurements of penicillin-induced activity (BAUMGARTNER *et al.*, 1989) suggest the existence of multiple independent sources. It can therefore be supposed that, by using an appropriate mathematical method, improved location and resolution of the underlying sources may be likely. There have been quantitative investigations into the certainty of source location and the spatial resolution of discrete (SHAOFEN *et al.*, 1990, LÜTKENHÖNER, 1994; OGURA and SEKIHARA, 1993) and distributed (GREENBLATT, 1993) sources for application in the human field. However, such systematic investigations for experimental studies on much smaller source volumes have been, as yet, unknown.

2 Method

2.1 *Mathematical basis*

A theoretical foundation for the spatial filter method is given by the Gilbert–Backus theory (PARKER, 1977). In accordance with this theory, optimum filter coefficients are derived for each location of a defined source region depending on the orientation of a current source (current dipole, current quadrupole etc.). Here, the term 'optimum' means that oriented current sources are detected by the filter response proportional to their strength. It implies that portions of the MEG signal from other sources in the source region are cancelled out to the greatest possible extent. Against this background, we apply a spatial filter the derivation of which is based on the spatial covariance of the MEG signal. Accordingly, the filter response, for location $\vec{r}$ and orientation θ, is only different from zero if a current dipole source exists at $\vec{r}$ and if this dipole is oriented with θ.

First, we note some definitions that are used for the subsequent filter derivation. The lead-field $\vec{L}_i(\vec{r})$, for channel i of a measurement system with n channels, is calculated on the basis of the forward solution of the magnetic field. $\vec{L}_i(\vec{r})$ is defined by the approach $B_i = \vec{L}_i(\vec{r}) \cdot \vec{m}(\vec{r})$. Here, B_i is the signal of channel i, predicted by means of the volume conductor model, and $\vec{m}(\vec{r})$ is the dipole moment of the generating dipole. From $\vec{L}_i(\vec{r})$, $(i = 1, \ldots, n)$, the vector $\boldsymbol{L}_\theta(\vec{r})$ is determined, which is composed of the components of each $\vec{L}_i(\vec{r})$ onto the orientation θ. Consequently, the signal vector $\boldsymbol{B} = (B_1, B_2, \ldots, B_n)^T$ relates to the value of the moment of a dipole, with the orientation θ, as

$$\boldsymbol{B} = \boldsymbol{L}_\theta(\vec{r}) \cdot m(\vec{r}) \tag{1}$$

Apart from $\boldsymbol{B}$, we introduce $\vec{\boldsymbol{M}} = (M_1, M_2, \ldots, M_n)^T$ for the measured signal at a time instant. The measured signal at the time instant $t_j = j \cdot \Delta t$, $(j = 1 \ldots l)$, is correspondingly termed by $\vec{M}_j$ ($1/\Delta t$ is the sampling rate, l is the number of sampling points). Further, we use $\boldsymbol{M}$, which comprises the l column vectors $\vec{M}_j$. Then, the spatial sample covariance $\boldsymbol{C}$ is defined by $\boldsymbol{C} = (1/l)\boldsymbol{M}\boldsymbol{M}^T$.

Finally, we use $\vec{\boldsymbol{M}}^* = \boldsymbol{P}\vec{\boldsymbol{M}}$ and $\vec{\boldsymbol{L}}_\theta(\vec{r}) = \boldsymbol{P}\boldsymbol{L}_\theta(\vec{r})$, where the projection operator $\boldsymbol{P}$ is defined by $\boldsymbol{P}^T\boldsymbol{P} = \boldsymbol{C}^{-1}$. Projected data $\boldsymbol{M}^*$ are 'whitened', so that $\boldsymbol{C}^* = (1/l)\,\boldsymbol{M}^*\boldsymbol{M}^{T*} = \boldsymbol{I}$($\boldsymbol{I}$ – identity matrix). To obtain $\boldsymbol{P}$, the matrix $\boldsymbol{C}$ is decomposed according to $\boldsymbol{C} = \boldsymbol{U}\boldsymbol{D}^2\boldsymbol{U}^T$, i.e. an orthogonal basis $\boldsymbol{U}$ for $\vec{\boldsymbol{M}}$ is constructed. $\boldsymbol{U}$ consists of the normalised eigenvectors of $\boldsymbol{C}$, and $\boldsymbol{D}^2$ represents a diagonal matrix with the corresponding eigenvalues in ordered succession. From this decomposition, the matrix $\boldsymbol{P} = \boldsymbol{U}\boldsymbol{D}^{-1}\boldsymbol{U}^T$ is computed.

On the basis of the preceeding definitions, we write down the general approach of the spatial filter response as

$$F_\theta(\vec{r}) = \vec{\boldsymbol{M}}^T \cdot \boldsymbol{a}^\theta(\vec{r}) \tag{2}$$

Here, $\boldsymbol{a}^\theta(\vec{r})$ represents the vector of filter coefficients that are determined from the entire set of measurement data within the investigated time interval. The coefficients are estimated by minimising the variance $\boldsymbol{a}^{\theta^T}\boldsymbol{C}\boldsymbol{a}^\theta$ of the filter response of eqn. 2, under the constraint $\boldsymbol{L}_\theta^{*T}(\vec{r})\boldsymbol{a}^\theta(\vec{r}) = 1$. The constraint ensures the filter response to be an estimate of $m(\vec{r})$. Solving this optimisation problem according to the Lagrange method for $\boldsymbol{a}^\theta(\vec{r})$, we obtain

$$\boldsymbol{a}^{\theta^T}(r) = \frac{\boldsymbol{L}_\theta^T(\vec{r})\boldsymbol{C}^{-1}}{\boldsymbol{L}_\theta^T(\vec{r})\boldsymbol{C}^{-1}\boldsymbol{L}_\theta(\vec{r})}$$

and accordingly, for $F_\theta(\vec{r})$,

$$F(\vec{r})_\theta = \frac{\boldsymbol{L}_\theta^T(\vec{r})\boldsymbol{C}^{-1}\vec{\boldsymbol{M}}}{\boldsymbol{L}_\theta^T(\vec{r})\boldsymbol{C}^{-1}\boldsymbol{L}_\theta(\vec{r})} = \frac{\boldsymbol{L}_\theta^{*T}(\vec{r})\boldsymbol{M}^*}{\boldsymbol{L}_\theta^{*T}(\vec{r})\boldsymbol{L}_\theta^{*T}(\vec{r})} \tag{3}$$

Moreover, to show the underlying Dirac properties of eqn. 3, let $\boldsymbol{B}$ now be a signal generated by k independent current dipoles ($k < n$), which can be defined by co-ordinates $(\vec{r}', \theta')$ and the dipole moment $m(\vec{r}')$, for each dipole. That is, $\boldsymbol{B}$ is formed by summing up k individual signal vectors, each being associated with one out of the k generating single dipoles. Further, let white multichannel noise $\boldsymbol{n}$ be superimposed, so that $\vec{\boldsymbol{M}} = \boldsymbol{B} + \boldsymbol{n}$, with $E[\boldsymbol{n}\boldsymbol{n}^T] = \lambda^2 \cdot \boldsymbol{I}$ ($\boldsymbol{I}$ = identity matrix). As, for the covariance $\boldsymbol{C}^*$ of the transformed data, it holds that $\boldsymbol{C}^* = \boldsymbol{I}$ (see above), we can draw the following conclusions, if $\lambda \to 0$:

(i) Owing to the new basis, the measurement space is split into the signal space Ω_S and a noise space Ω_n. Ω_S is represented by k eigenvectors of $\boldsymbol{C}$ associated with the k greatest eigenvalues; Ω_n is represented by the other $n - k$ eigenvectors.
(ii) (*a*) After being transformed, the individual signal vectors are orthogonal to each other. Therefore, the contribution of a current dipole, with co-ordinates $(\vec{r}', \theta')$, to the measured signal is extracted by $F_\theta(\vec{r})$, if $(\vec{r}, \theta) = (\vec{r}', \theta')$. Moreover, the filter response results in $m(\vec{r}')$ because of the linear relationship of eqn. 1.
(*b*) The transformed signal vector $\boldsymbol{L}_\theta^*(\vec{r})$ of any unity dipole source, with $\vec{r} \neq \vec{r}'$, lies within this noise subspace. Further, for the same signal vector, it follows that $\|\boldsymbol{L}_\theta^*(\vec{r})\| \to 1/\lambda\|\boldsymbol{L}_\theta(\vec{r})\|$.
(*c*) For $\vec{r} = \vec{r}'$ and $\theta \neq \theta'$, there is a component of $\boldsymbol{L}_\theta(\vec{r})$ (orthogonal to $\boldsymbol{L}_{\theta'}(\vec{r})$) that is also transformed into the noise space. As the norm of the transformed component and therefore of $\boldsymbol{L}_\theta^*(\vec{r})$ tends to infinity, $\boldsymbol{L}_\theta^*(\vec{r})$ is also an element of the noise space.

Thus, all $\boldsymbol{L}_\theta^*(\vec{r})$, with $(\vec{r}, \theta) \neq (\vec{r}', \theta')$ lie within the noise space and are therefore orthogonal to the vector $\vec{\boldsymbol{M}}^*$.
(iii) Consequently, from these considerations, together with eqn. 3, we obtain:

$$F_\theta(\vec{r}) = \begin{cases} m(\vec{r}'), & (\vec{r}, \theta) = (\vec{r}', \theta') \\ 0, & (\vec{r}, \theta) \neq (\vec{r}', \theta') \end{cases}$$

To assess quantitatively the quality of both location and resolution that is obtainable using eqn. 3, we introduce other specific eqns. 4 and 5.

An active region of nerve cells within the cerebral cortex exhibits laminar structure (MITZDORF, 1985). Further, intracellular currents that account for the origin of the external magnetic field have predominantly fixed orientations (MITZDORF, 1985), i.e. the spatial angle subtended by potential rotating dipoles is negligibly small.

On the basis of this neuro-electric background, we note the following expressions:

To locate sources, we use the variance equation (dimensionless)

$$F_\theta(\vec{r}) = \frac{1}{s_0} \cdot \frac{L_\theta^T(\vec{r}) L_\theta(\vec{r})}{L_\theta^T(\vec{r}) C^{-1} L_\theta(\vec{r})} \tag{4}$$

(s_0 is a normalisation factor; it equals the variance of the measurement signal).

This expression is closely related to eqn. 3. From eqn. 3 it can be derived that the denominator in eqn. 4, $L_\theta^T(\vec{r})C^{-1}L_\theta(\vec{r})$, equals the reciprocal variance of the filter response eqn. 3. Therefore, and with respect to eqn. 1, $F_\theta(\vec{r}) \cdot s_0$ leads to the portion of the signal variance that is accounted for by a current dipole located at $\vec{r}$ and oriented with θ. Provided the signal originates from a single dipole source, with co-ordinates $(\vec{r}', \theta')$ and arbitrary dipole moment, then it follows that

$$F_\theta(\vec{r}) = \begin{cases} 1, & (\vec{r}, \theta) = (\vec{r}', \theta') \\ 0, & (\vec{r}, \theta) \neq (\vec{r}', \theta') \end{cases}$$

i.e. eqn. 4 is suitable for locating dipole sources.

If the biomagnetic signal is generated by point sources, then the co-ordinates and orientations of generating sources are determined by the maxima of $F_\theta(\vec{r})$.

Eqn. 4 also admits another interpretation: the right-hand side of eqn. 4 can be thought to be a measure of the projection of the signal space associated with the dipole probe onto the space of the measurement signal*. Based on this interpretation, we apply the subsequent matrix to the assessment and improvement of the resolution of closely adjacent sources $Q_{\theta_1,\theta_2}(\vec{r}, \vec{a}) = U_{\theta_1,\theta_2}^T(\vec{r}, \vec{a}) C^{-1} U_{\theta_1,\theta_2}(\vec{r}, \vec{a})$ (see also GREENBLATT (1993)).

Whereas eqn. 4 refers to a single dipole probe, $Q_{\theta_1,\theta_2}(\vec{r}, \vec{a})$ is obtained by extending eqn. 4 to a probe consisting of two current dipoles. It is suited to detecting the location and orientation parameters of adjacent dipoles. $\vec{a}$ denotes the relative position of the two dipoles, and θ_1 and θ_2 denote their orientations. The location of this pair of dipoles is defined by $\vec{r}$, which is calculated from $\vec{r} = 0.5(\vec{r}_1 + \vec{r}_2)$, where $\vec{r}_1$ and $\vec{r}_2$ represent the location of the individual dipoles. $U_{\theta_1,\theta_2}(\vec{r}, \vec{a})$ represents the system of eigenvectors that spans the signal space of the two dipole probe (details of constructing $U_{\theta_1,\theta_2}(\vec{r}, \vec{a})$ can be seen in the Appendix). These eigenvectors are projected into the measurement signal space according to $U_{\theta_1,\theta_2}^*(\vec{r}, \vec{a}) = PU_{\theta_1,\theta_2}(\vec{r}, \vec{a})$, ($P = C^{-1/2}$). To obtain a projection measure, the product $U_{\theta_1,\theta_2}^{*T}(\vec{r}, \vec{a}) U_{\theta_1,\theta_2}^*(\vec{r}, \vec{a}) = Q_{\theta_1,\theta_2}(\vec{r}, \vec{a})$ is used. Then, the projection measure $M_{\theta_1,\theta_2}(\vec{r}, \vec{a})$ is calculated by means of

$$M_{\theta_1,\theta_2}(\vec{r}, \vec{a}) = \frac{1}{s_0} trace[Q_{\theta_1,\theta_2}^{-1}(\vec{r}, \vec{a})] \tag{5}$$

(matrix $Q_{\theta_1,\theta_2}(\vec{r}, \vec{a})$ has to be inverted because of the 'whitening' effect of P).

* Then, the assumption of independent generators can be dropped.

2.2 *Instrumentation, volume conductor model, source model*

The numerical simulation of source analysis is performed with reference to the actual experimental conditions: MEG measurement is carried out by means of a seven-channel gradiometer (Fig. 1*a*). By changing the location of the subject below the gradiometer in a definite way, 21- and 35- channel devices can be simulated (Fig. 1*b*).

For the volume conductor model, a sphere with homogeneous conductivity is chosen. In the present case of interictal spike activity, the current sources are close to the surface of the cortex. Therefore it can be assumed that, for source analysis of real MEG data, the spherical model of the volume conductor offers a good approximation (see also PETERS and DE MUNCK (1990)). The distance of the centre of the modelling sphere from the measurement plane amounts to 30 mm: this value was found to be realistic for the cortex of the rabbit. The calculation of the magnetic field strength is accomplished according to the formulas given by STOK (1986).

For the computer simulation, the centre of the source region is placed 12.8 mm below the measurement plane. Its spatial extension is 10 × 10 mm horizontally and 3.5 mm in a vertical direction. The distance of the surface of the sphere from the top of the source region is assumed to be 1 mm.

During the study of the resolution of sources, the source region is subdivided into horizontal slices of 0.5 mm thickness, respectively. Each slice consists of 400 voxels.

A finer segmentation of the source region is necessary for studying the certainty of location. Then, the thickness of a slice amounts to 0.1 mm. Conversely, the horizontal extension can be reduced to 3 × 3 mm, so that the number of the voxels in each slice is 900. In the source analysis, the filter coefficients are computed for the centre of each voxel.

To generate simulated MEG data by means of discrete source models, i.e. single or multiple current dipoles, magnetic fluxes through the gradiometer coils are calculated. Furthermore, white noise is superimposed as noise signal onto these fluxes according to a given signal–noise ratio (SNR); we relate the SNR to the maximum, absolute amplitude of the undisturbed B field.

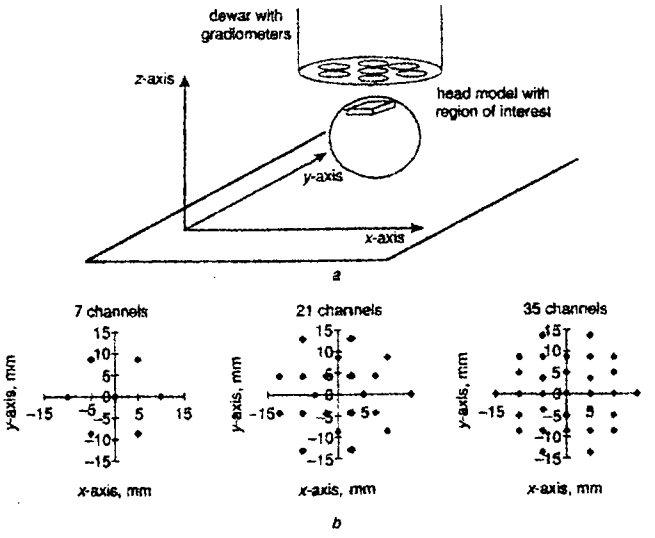

Fig. 1 *(a) Schematic representation of the seven-channel measurement system used, with spherical volume conductor and reference-system axes. The reference-system origin is determined by point on the sphere surface nearest to the measurement plane. (b) Positions of pick-up coils of seven-channel system and simulated 21- and 35-channel systems*

In the case of noisy MEG data, the resolution of adjacent current dipoles depends greatly on the relationship between the temporal courses of the dipole moments. For linearly dependent sources the resolution clearly decreases. On the other hand, the knowledge of the exact temporal course of the moment of a real dipole source is not so important with respect to the resolution of sources. Therefore, in our studies we need not simulate the biphasic course of epileptical spike activity exactly. As the aim of this work is to deal with the resolution of two independent sources we have chosen two orthogonal harmonic functions. These functions cover one and two periods, respectively, in the interval analysed (duration of the interval = 128 time points).

The algorithm of the spatial filter was developed with the aid of a PC and is programmed in Microsoft C language, version 7.0.

3 Results

To examine the accuracy of source location obtainable using eqn. 3, the algorithm in eqn. 4 is applied. The magnetic field is generated by an equivalent dipole. This is placed 2 mm beneath the surface of the sphere, with tangential orientation. The co-ordinates associated with maximum filter response are interpreted as the estimated position of the current dipole. By repeated simulation (100 times), information about the accuracy of location denoted by mean value and standard deviation of the spatial co-ordinates is obtained. The result of this estimation, which is dependent on the number of channels and the SNR, is demonstrated in Fig. 2. The bias of estimation is small, i.e. the position of the current source is correctly estimated. The uncertainty of a single estimation of the x-coordinate of the source location, on the basis of a seven-channel system and an SNR of 5 : 1, is found to be 0.2 mm. This quantity is nearly twice as much for the z-coordinate. By means of a 21- and a 35-channel system, respectively, and the same SNR of 5 : 1, the reduction of this inaccuracy for both x and y is small.

In Fig. 3, an instantaneous view of the filter response (eqn. 3) to a magnetic field (SNR = 50 : 1) is shown. This field is generated by two independent current dipoles placed along the y-axis with a distance of 4 mm and oriented parallel to the x-axis. The location of both sources is exactly reflected in the plane of the sources (middle plane). However, in the slice above the source plane, the sources seem to diverge and, in the slice below the source plane, they seem to converge. This is

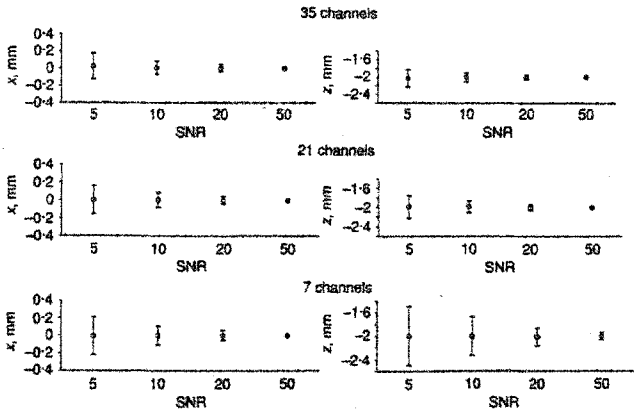

Fig. 2 *Representation of accuracy (described by estimated x- and z-co-ordinates and their standard deviations s_x and s_z) of locating a single dipole source, having local co-ordinates [0, 1, −2] and orientation [1, 0, 0] against SNR and the number of channels (s_y < 0.1 mm). Number of trials = 100.*

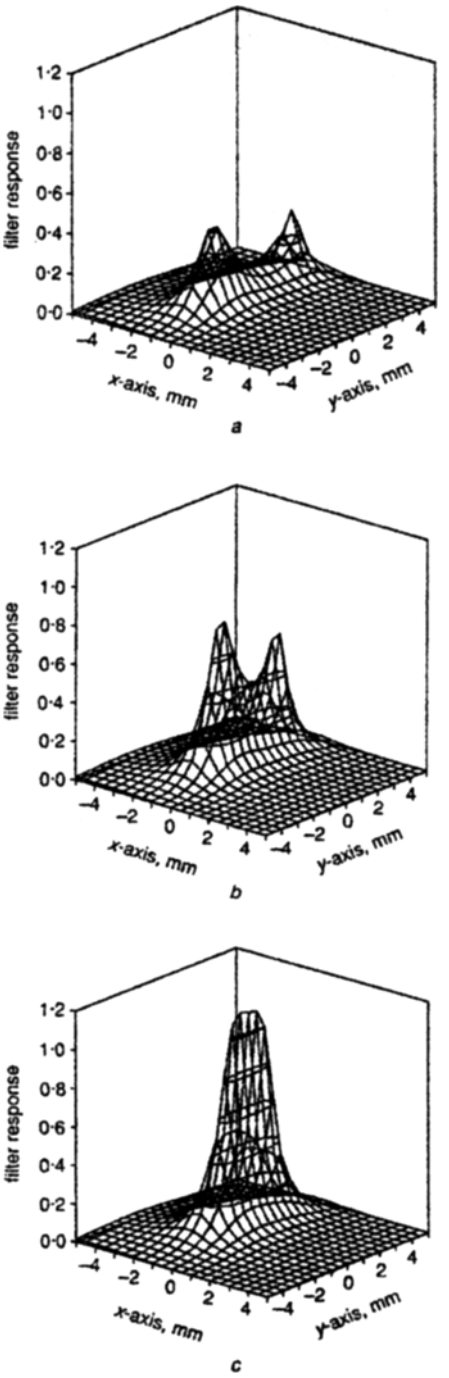

Fig. 3 *Instantaneous filter response of two current dipoles calculated according to eqn. 3 in three horizontal planes of the source region. The dipoles are at a distance of 4 mm and have co-ordinates of [−1, −1, −1] and [−1, 3, −1], respectively, and the orientation [1, 0, 0]. The source plane is at a depth of 1 mm. ○ (a) depth = 0.5 m; (b) depth = 1.0 mm; (c) depth = 1.5 mm*

owing to the disturbance of the 'measured magnetic field' by noise. Thus, if the depth is unknown, the assignment of the sources to a certain depth and also their location in a horizontal plane are impaired. Therefore, eqn. 5† is used to

† Matrix Q from eqn. 5 differs principally from the (2,2) matrix of GREENBLATT (1993) for a spherical volume conductor. Greenblatt has introduced a projection measure for a rotating dipole that is used as a weighting factor in the inverse problem of the current dipole field. Unlike this author, using eqn. 5, we formulate a means of calculating the projection measure of the summed-up field of two locally separated dipoles.

resolve closely adjacent sources instead of the filter eqn. 3. The analysis is performed on the basis of a source model consisting of two current dipoles. For this model, typical two-dipole arrangements are selected by which different results for the problem of resolution are to be expected.

Both dipoles have local coordinates $[-0.5d, 1, -2]$ and $[0.5d, 1, -2]$ (case 1); $[0, -0.25d, -2]$ and $[0, 0.75d, -2]$ (case 2); or $[0, 1, 0.5d-2]$ and $[0, 1, -0.5d-2]$ (case 3); i.e. the straight line between the sources is parallel to one of the axes of the co-ordinate system. The vectors of current dipoles lie in a horizontal plane, and the amplitude of their moments amounts to unity. The distance between the dipoles is denoted by d. Furthermore, in all cases, both dipoles of the source model have orientations parallel to the x-axis. We term the arrangement of the dipoles linear for case 1, and parallel for case 2 or case 3. Accordingly, the matrix underlying eqn. 5 is calculated with the constraint that the probe dipoles are oriented in parallel.

The location analysis of a magnetic field generated by the two-dipole source for $d = 2$ mm is carried out. For this purpose, we define a parameter d' by $d' = \|\vec{a}\|$, the parameter d' being the dipole distance of the probe dipoles from each other (for $\vec{a}$, see explanation for eqn. 5). For fixed d', eqn. 5 is evaluated at each point of the source region, as described in Section 2.1. Then, the maximum of $M_{\theta_1,\theta_2}(\vec{r}, \vec{a})$ for fixed d' is noted. Further, for d', a range of 0–4 mm in steps of 1 mm is chosen. Thus, the maximum value depending on d' is studied. Ultimately, the d' that yields maximum $M_{\theta_1,\theta_2}(\vec{r}, \vec{a})$ is chosen as the estimated d.

As seen from Fig. 4, the course of $M_{\theta_1,\theta_2}(\vec{r}, \vec{a})$ differs only slightly for $d' = 0$, 1, 2, 3. However, within the ensemble of these four curves, one curve ($d' = 2$ mm) with maximum $M_{\theta_1,\theta_2}(\vec{r}, \vec{a})$ is recognisable.

The certainty of the estimated source model parameters (location and distance of the two dipoles) was examined by repeated calculations. In Fig. 5, the result of computation experiments for adjacent sources separated by $d = 2$ mm is shown for a 35-channel system depending on SNR. Here, as a result of examining cases 1 and 2, an optimum determination of the source model parameters is to be expected if the dipole sources are positioned along the y-axis (case 2, Fig. 5*b*). Thus, for SNR $\geq 20:1$, we obtain a standard deviation for d of 0.5 mm. The situation is more unfavourable in the case of sources that are positioned along the x-axis (case 1, Fig. 5*a*). In

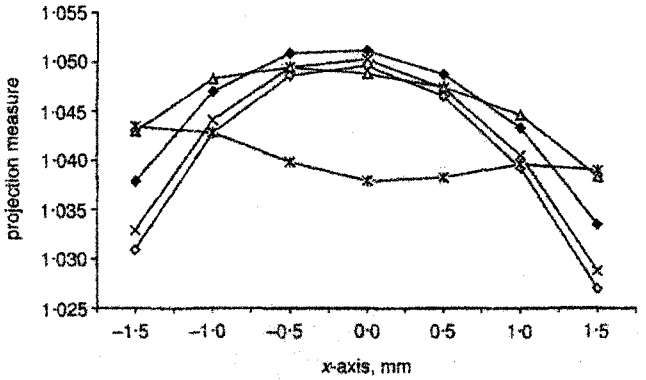

Fig. 4 *Location analysis, using eqn. 5 of registered field of two current dipoles positioned at [−1, 1, −2] and [1, 1, −2] and oriented parallel to the x-axis against given distance parameter d′ (see text). SNR = 50 : 1; channel number = 35. The result of the analysis is represented for the source plane along a straight line between both dipoles. (◇) d′ = 0 mm; (−✱−) d′ = 1 mm; (−◆−) d′ = 2 mm; (△) d′ = 3 mm; (−✱−) d′ = 4 mm*

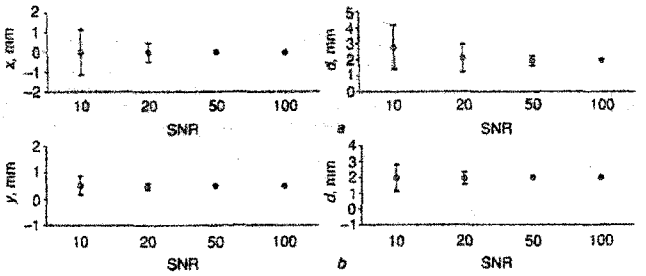

Fig. 5 *Results of repeated locating experiments (100 times) against SNR. Two generating parallel dipoles are separated by 2 mm. The dipoles point in the x-direction. Channel number = 35. (a) Position of sources: [−1, 1, −2] and [1, 1, −2]; the result of locating is described by the estimated mean distance d of the dipoles, the estimated mean x-co-ordinate of the dipole pair and the standard deviations s_d and s_x. For s_y and s_z values < 0.2 mm were found. (b) Position of sources: [0, −0.5, −2] and [0, 1.5, −2]; the result of locating is described by the estimated mean distance d of the dipoles, the estimated mean y-co-ordinate of the dipole pair and the standard deviations s_d and s_y. For s_x and s_z values < 0.2 mm were found*

that case, an SNR $\geq 50:1$ is required to obtain the same certainty for d as in case 2. In case 3, where the sources are positioned along the z-axis, the determination of d appears to be still more uncertain. SNR $\geq 100:1$ is then necessary to obtain a certainty for d similar to that in case 2, for SNR $\geq 20:1$.

Further, to check the power of resolving two sources (we restrict ourselves to case 2), a measure F according to the formula eqn. 6 is proposed

$$F = \frac{\Sigma_1 - \Sigma_2}{\Sigma_2} \cdot \frac{n_2}{n_1 - n_2} \tag{6}$$

where Σ_1 is the residual sum of squares obtained on the basis of a single dipole model, and Σ_2 is the residual sum of squares on the basis of a two dipole model; n_1 and n_2 are the respective degrees of freedom‡. In Fig. 6 F-histograms for various SNRs derived from 1000 samples for each curve are shown. The solid lines result from F-calculations using simulated measurements generated by a single dipole, whereas the broken lines result from measurements generated by two dipoles separated by 2 mm. As mentioned above, for SNR = 20 : 1, the standard deviation of d is small (0.5 mm). However, Fig. 6*a* indicates a poor resolution. This resolution has clearly improved for SNR = 30 : 1 (Fig. 6*b*). From this finding we conclude:

(i) for $F \geq 9.1$ calculated, the two parallel dipole sources can be considered to be separable with an α-error $\leq 1\%$
(ii) assuming $F < 9.1$ calculated and SNR $\geq 30:1$, the resolution of the two sources can be rejected with a β-error $\leq 7.5\%$, if the distance d of the actual sources is ≥ 2 mm.

4 Discussion

Simulation by current models is performed throughout with current dipoles oriented in the horizontal direction. This orientation was chosen because, in a volume conductor with

‡ The measure F formally corresponds to the F-statistic in the least squares technique (WINER, 1971). The source amplitudes at each time point are calculated by linear regression for a set of source co-ordinates and orientations found by spatial filtering.

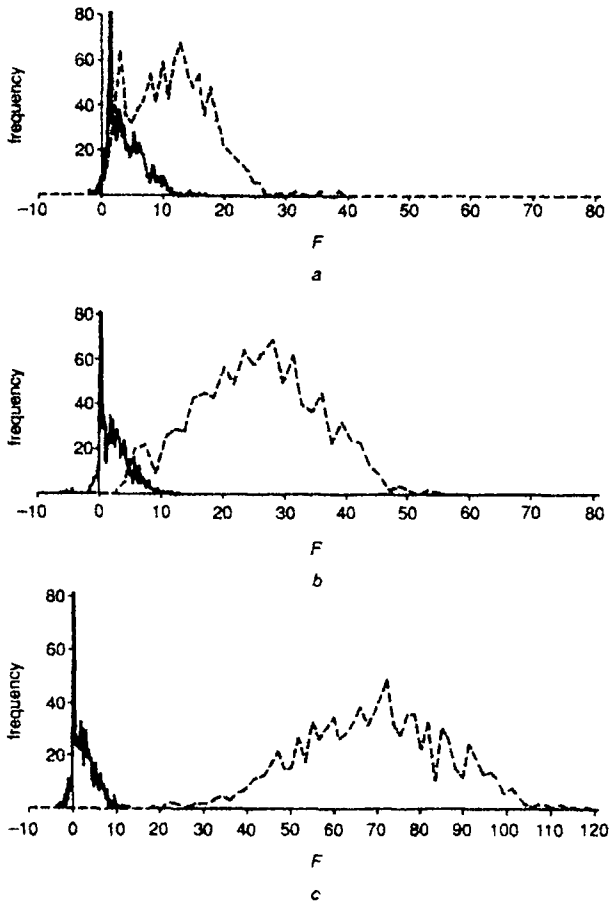

Fig. 6 *F-histograms for resolution of two independent dipole sources with aid of spatial filter method (eqn. 5). Dipole sources are placed along straight line parallel to y-axis at depth of 2 mm; positions of current dipoles: [0, −0.5, −2] and [0, 1.5, −2], orientations parallel to x-axis; number of channels: 35; total sample number of each histogram: 1000. (a) SNR = 20:1; (b) SNR = 30:1; (c) SNR = 50:1. (- - -)F-histogram calculated for single dipole generator; peak frequency values: (a) 152; (b) 159; (c) 176. (—) F-histogram calculated for two generating dipoles (d = 2 mm).*

a spherical shape, radial dipoles do not contribute anything to the external magnetic field. Conversely, in the cerebral cortex, intracellular currents are mainly oriented perpendicular to the cortical surface. For a detailed investigation of intracortical neuronal processes during epileptiform spike generation the rabbit brain is favourable. The cortex is smooth and unfolded (lissencephalic), but with parts (medial cingulate cortex) arranged tangentially to the brain surface. Hence, to realise the generation of tangential current components, the injection of penicillin is implemented at the medial cingulate cortex of the rabbit.

In comparison with the location of a single source, the spatial resolution of closely adjacent and equally oriented current sources requires a significantly higher quality of measurement. This quality mainly depends on the SNR. The best resolution is found if the current dipoles are parallel, in a horizontal plane (case 2). If the current dipoles are linearly arranged (case 1) the resolution deteriorates. This can be explained by the fact that, even with a greater distance between the sources, the measured magnetic field may be identical to that of a single equivalent dipole. Then, the temporal course of the moment of this dipole is constituted by the sum of the dipole moments of the individual sources at each instant. In the case of vertically arranged sources (case 3), a further deterioration of resolution is to be observed, as with the uncertainty of the z-co-ordinate of a single dipole.

Parallel or antiparallel current dipoles are relevant source models in the cerebral cortex of the species of current interest (rabbit). In other species with a folded cortical surface (gyrencephalic brain, e.g. the human brain), other arrangements might be of importance that are different from the parallel orientation of the dipoles.

The strategy of resolution of sources on the basis of a pair of dipoles as a probe unit significantly differs from the common practice of spatial filtering with a single dipole probe. It enables us to resolve closely adjacent sources and to determine their parameters quantitatively.

To summarise, we can derive the following from the preceding theoretical investigations:

(i) Location of a single current source by means of a spatial filter may be feasible with an accuracy of < 0.5 mm, provided that an SNR of 5:1 can be obtained by averaging individual measurements.
(ii) The resolution of adjacent sources is sensitive to the mutual location of these sources and their orientation. Although the results of SVD might suggest the existence of several sources, a reliable identification of these sources is only ensured for SNR > 20:1. Thus, for a parallel arrangement of two independent current dipoles lying in a horizontal plane, a resolution of 2 mm is found for an SNR of 30:1.

Acknowledgment—The authors wish to thank Dr D. Kaiser from the Department of Applied Mathematics at the Friedrich Schiller University for placing an SVD routine at their disposal and for helpful discussions on numerical problems.

This work was Supported by the German Bundesministerium für Bildung und Forschung (project 01 ZZ 9104).

References

ACHIM, A., RICHTER, F., and SAINT-HILAIRE, J.M. (1991): 'Methodological considerations for the evaluation of spatio-temporal source models', *Electroenceph. Clin. Neurophysiol.*, **79**, pp. 227–240

BAUMGARTNER, Ch., SUTHERLING, W.W., DI, S., and BARTH, D.S. (1989): 'Investigation of multiple simultaneously active brain sources in the electroencephalogram', *J. Neurosci. Methods*, **30**, pp. 175–184

BAUMGARTNER, Ch., SUTHERLING, W.W., DI, S., and BARTH, D.S. (1991): 'Spatiotemporal modeling of cerebral evoked magnetic fields to median nerve stimulation', *Electroenceph. Clin. Neurophysiol.*, **79**, pp. 27–35

FUCHS, M., WAGNER, M., WISCHMANN, H.A., and DÖSSEL, O. (1995): 'Cortical current imaging: a new approach for MEG-reconstructions', *in* Eiselt, M., Zwiener, U., and Witte, H. (Eds): 'Quantitative and topological EEG and MEG analysis' (Universitätsverlag Jena) pp. 77–81

GOLDENSOHN, E.S., and SALAZAR, A.M. (1986): 'Temporal and spatial distribution of intracellular potentials during generation and spread of epileptogenic discharges', *in* DELGADO-ESCUETA, A.V., WARD, A.A., WOODBURY, D.M., and PORTER, R.J. (Eds.): 'Advances in neurology. (Raven Press, New York) pp. 559–589

GREENBLATT, R.E. (1993): 'Probabilistic reconstruction of multiple sources in the bioelectromagnetic inverse problem', *Inverse Prob.*, **9**, pp. 271–284

GRUMMICH, P., KOBER, H., and VIETH, J. (1992): 'Localization of the underlying currents of magnetic brain activity using spatial filtering', *Biomed. Eng. (Berlin)*, **37**, pp. 158–159

IOANNIDES, A.A., BOLTON, J.B., and CLARKE, C.J.S. (1990): 'Continuous probabilistic solutions to the biomagnetic inverse problem', *Inverse Prob.*, **6**, pp. 523–542

LÜTKENHÖNER, B. (1995): 'Dipole and multidipole source analysis of magnetic fields: Possibilities and limitations'. *in*: DEECKE, L., and

BAUMGARTNER, C. (Eds.): 'Proceedings of the 9th International Conference on Biomagnetism' (Elsevier, Amsterdam) pp. 376–380
MITZDORF, U. (1985): 'Current source-density method and application in cat cerebral cortex: investigation of evoked potentials and EEG phenomena', *Physiol. Rev.*, **65**, pp. 37–100
MOSHER, J.C., SPENCER, M.E., LEAHY, R.M., and LEWIS, P.S. (1993): 'Error bounds for EEG and MEG dipole source localisation', *Electroenceph. Clin. Neurophysiol*, **86**, pp. 303–321
OGURA, Y., and SEKIHARA, K. (1993): 'Relationship between dipole parameter estimation errors and measure conditions in magnetoencephalography', *IEEE Trans.*, **BME-40**, pp. 919–924
OKADA, Y. (1985): 'Discrimination of localized and distributed current dipole sources and localized single and multiple sources
In: Weinberg, U., Stroink, G., Katila, T. (eds.) Biomagnetism: Application and Theory, Pergamon Press, New York, pp. 266–272
PARKER, R.L. (1977): 'Understanding Inverse Theory', ANN. Rev. Earth Planet. Sci., **5**, pp. 35–64
PASCUAL-MARQUI, R.D., MICHEL, C.M., and LEHMANN, D. (1994): 'Low Resolution Electromagnetic Tomography: A New Method for Localizing Electrical Activity in the Brain', *Int. J. Psychophysiol.* , **18**, pp. 49–65
PETERS, M., DE MUNCK, J. (1990): 'On the Forward and the Inverse Problem for EEG and MEG' In: Grandori, F., Hoke, M., Romani, G. L. (eds.): 'Auditory Evoked Magnetic Fields and Electric Potentials.', Adv. Audiol., Karger, Basel, **6**, pp. 70–102
ROBINSON, S.E., and ROSE, D. (1992): 'Current Source Image Estimation By Spatially Filtered MEG' In: Hoke, M., Erné, S., N., Okada, J. C., Romani, G.L. (eds.): 'Biomagnetism: Clinical Aspects, (Excerpta Medica, Amsterdam)', pp. 337–378
SHAOFEN, T., BRADLEY, J.R., and WIKSWO, J.P., JR. (1990): 'The magnetic field of cortical current sources: The application of a spatialfiltering model to the forward and inverse problems', *Electroenceph. Clin. Neurophysiol.*, **76**, pp. 73–85
STOICA, P., and NEHORAI, A. (1989): 'MUSIC, maximum likelihood and Cramer-Rao bound', IEEE Trans. ASSP, **37**, pp. 720–741
STOK, C. J. (1986): 'The inverse problem in EEG and MEG with application to visual evoked responses' (Krisp Repro Meppel, Leiden)
WANG, J.Z., KAUFMANN, L., and WILLIAMSON, S.J. (1993): 'Imaging regional changes in the spontaneous activity of the brain: an extension of the minimum-norm least-squares estimate', *Electroenceph. Clin. Neurophysiol.*, **86**, pp. 36–50
WINER, B.J. (1971): 'Statistical principles in experimental design' (McGraw-Hill Kogakusha, Ltd.), p.139

Appendix

Between the vector of the dipole moments $\boldsymbol{q} = (q_1, q_2 \ldots q_m)^T$ of m fictive current dipoles $q_i (i = 1 \ldots m)$ in the source region and the external, undisturbed magnetic induction $\boldsymbol{B} = (B_1, B_2 \ldots B_n)^T$, which is generated by these dipoles and registered in n pickup coils of a magnetometer, the linear relationship

$$\boldsymbol{B} = \boldsymbol{L}\boldsymbol{q} \tag{7}$$

holds, where the elements l_{ij} of the matrix $\boldsymbol{L}$ are the response of the pickup coil i to the dipole j with unity dipole moment.

According to eqn. 7, the vector space of $\boldsymbol{B}$ is spanned by the column vectors of $\boldsymbol{L}$. Instead of $\boldsymbol{L}$, we introduce a new, orthonormal basis $\boldsymbol{U}$, which is obtained by spectral decomposition of the matrix $\boldsymbol{L}$ according to $\boldsymbol{L} = \boldsymbol{U}\boldsymbol{D}\boldsymbol{Q}^T$, with the orthonormal matrices $\boldsymbol{U}(n, m)$ and $\boldsymbol{Q}(m, m)$, $n > m$ and the diagonal matrix $\boldsymbol{D}$.

Authors' Biographies

Hans Wagner was born in Jena, Germany, in 1936. He graduated in Physics from the Friedrich Schiller University of Jena. Since 1969, he has been working on the field of biomedical research at the Medical Faculty of the same university. He received the Ph.D in 1975, on the subject of the mathematical analysis of tracerkinetic data. Since 1978, he has dealt with time-series analysis of EEG and cardiorespiratory signals. His current research interests include the localisation of brain electric sources by analysis of EEG and MEG signals.

Michael Eiselt was born in Gera, Germany, in 1956. He received the Medical Diploma, in 1983, and the MD degree, in 1987, from the Friedrich Schiller University of Jena. In 1987 he received the Specialisation in Pathophysiology. His research interests include clinical and experimental neurophysiology, with special regard to epilepsy. Since 1991, he has worked on problems of the generation and spread of epileptic seizures detected by EEG and MEG.

Ulrich Zweiner was born in Schweina, Germany in 1942. He received the MD degree, in 1967, the specialization in Pathophysiology in 1967, and graduated as a Docor of Sciences in 1974. He received a Ph. D. from the Humboldt University of Berlin in 1975. Since 1978 he has been Professor and Chairman of the Insitute of Pathophysiology of the Friedrich Schiller University of Jena. Since 1967, he has dealt with the pathophysiology of the autonomous nervous system and cerebral electrophysiology.